Discordant expression profile between RNA and protein for the genes involved in immune response network in adenovirus type 2 infected cells

Hongxing Zhao*, Maoshan Chen[1], Alberto Valdés[2], Sara Bergström Lind[2], and Ulf Pettersson

Dept. of Immunology, Genetics and Pathology, Uppsala University, S-751 85 Uppsala, Sweden.

[1]Department of Biochemistry and Genetics, La Trobe Institute for Molecular Science, La Trobe University, Melbourne, Victoria 3086, Australia.

[2]Department of Chemistry-BMC, Analytical Chemistry, Uppsala University, Box 599, SE-751 24 Uppsala, Sweden

*Corresponding author:

E-mail address: Hongxing.Zhao@igp.uu.se (H. Zhao).

Fax: +46 18 471 4808.

Running title: Gene expression profile in Ad2-infected cells

197 words in the abstract

6314 words for the text

Abstract

Alternation of cellular genes expressions during Adenovirus type 2 (Ad2) infection in IMR-90 cells was studied using paired-end sequencing and stable isotope labeling of amino acids in cell culture mass spectrometric analysis (SILAC-MS). At transcriptional level, cellular genes involved in different pathways revealed distinct expression profiles. At early phase, the genes involved in regulation of cellular immune response, cellular signaling and cell growth control were among the most deregulated. Later follows, in an orderly fashion, genes involved in cell cycle control, DNA replication and further on genes engaged in RNA processing and protein translation. Comparison of cellular gene expression at transcriptional and posttranscriptional levels revealed low correlation. Here we highlight the genes which expose opposite expression profiles with an emphasis on key factors that play important roles in cellular immune pathways including NFκB, JAK/STAT, caspases and MAVS. Transcription of many of these genes was transiently induced early, but became down-regulated in the late phase. In contrast, their expressions at protein level were up-regulated early and so sustained until late phase of infection. Suppression at the transcriptional level and enhancement at the protein level of immune response genes most likely illustrate counteractions between Ad2 and its host cell.

Importance

Our paper comprises a state of the art quality transcriptomics data set unravelling the alterations in gene expression that take place during different phases of an adenovirus infection. The information allows us to draw conclusion about the cellular pathways that are perturbed by the virus. The data set also provides an important resource for scientists in general for future studies on mechanisms behind host/virus interactions in efforts to design tools for combatting virus infections.

Moreover, our paper includes novel proteomics information unravelling an unexpected role of post transcriptional events in cellular gene expression, demonstrating that the current picture of the adenovirus replication cycle is simplified.

Introduction

Human adenovirus (Ad) infection leads to alternations of host cell gene expression and biosynthetic processes. It is a stepwise, but efficient mode of turning host transcriptional, translation and metabolism to facilitate the replication of adenovirus. Most interactions between host cell and virus take place during the early phase. Adenovirus-mediated regulation of cellular gene expression emphasizes two major aspects: interference with host defense mechanisms and induction of its host cell to enter S-phase of the cell cycle. It has also been shown that cells are reprogrammed epigenetically as a result of adenovirus early-region function at different times after infection (1). Adenovirus expresses several regulatory proteins from early regions 1A (E1A), E1B, E3, and E4. E1A is the first viral gene expressed and plays essential roles in regulation of viral and cellular genes expression (2). E1A proteins are crucial for the induction of the S phase of the cell cycle, cell proliferation and cell transformation through its ability to target different cellular transcriptional regulators, such as pRb, p300/CBP, CtBP, p400/TRRAP (3-10). E1A proteins also interfere with host immune response by blocking type I IFN-inducible gene expression (11), as well as by preventing the peptide presentation to the immunoproteosome by interacting with MECL1 (12). E1B encodes two major proteins, the E1B-55K and E1B-19K proteins. E1B-55K is a multi-functional protein and plays a major role in counteracting the cellular proapoptotic program. Association of E1B-55k and E4 orf6 proteins with several cellular proteins, Cullin 5, TCEBs and RBX1 forms a virus-specific E3 ubiquitin ligase which then targets specific cellular proteins for degradation (13). The E1B-55K protein serves as the substrate-recognition subunit via distinct sequences and targets the p53 protein, thereby promoting degradation of p53 (14, 15). The E1B-19K protein is a viral Bcl-2 homologue that acts as a broad inhibitor of mitochondria-dependent apoptosis (16, 17). It interferes directly with the activity of p53 when translocated into the mitochondria (18). Proteins generated from the E3 region also play a

very important role in countering host antiviral defenses (19). E3-gp19K prevents the exposure of viral peptides on the cell surface by blocking the transport of the class I major histocompatibility complex (MHC I) molecule to the cell surface and the loading of peptides by tapasin (20-22). The E3-10.4K and 14.5K (RIDα/β) complex inhibits tumor necrosis factor alpha (TNFα) and Fas ligand-induced apoptosis through internalization and degradation of the death domain containing receptors (23). In addition, the E3-10.4K/14.5K complex blocks the activation of NFκB by preventing it from entering the nucleus and inhibiting the activity of the kinase complex IKK (24). Proteins encoded by the E4 region are involved in transcriptional regulation. E4 orf6/7 stabilizes the binding of E2F to the duplicated E2F binding sites in the E2 promoter (25, 26). E4 orf3 associates with E1B 55K in the nuclear promyelocytic leukemia protein oncogenic domains (POD) and reorganizes PODs during infection, thus likely involved in the regulation of transcription factor availability and activity (27). The E4 orf4 protein interacts with protein phosphatase 2A, leading to the inhibition of E1A-dependent transactivation of the junB promoter (28).

When adenovirus DNA replication commences, the infection cycle proceeds into the late phase and viral transcription changes from the early to the late pattern. E1A expression switches from a preference for the 289R transcriptional activator to the shorter E1A-243R protein (29). The E1A-243R protein functions mainly as a transcriptional repressor through its binding of p300/CBP (30). The L4-100 kDa protein, expressed from the major late transcription unit is necessary for efficient initiation of viral late mRNA translation (31-33). Furthermore, the E1B-55 kDa and E4 orf4 protein complex is involved in regulation of mRNA export from nucleus, resulting in a block of cellular mRNAs export and selective export of viral mRNAs (34, 35). As a consequence a dramatic down-regulation of cellular gene expression occurs late in infection (36).

Most studies of the adenovirus infection have been performed in Hela cells, in which adenovirus replication is very efficient and the infectious cycle is completed after 20-24 hours. Particularly, the early phase is very short, lasting for less than 6 hours. Thus, there is a narrow time window for a detailed examination of the changes of cellular gene expression. Furthermore, being transformed cells, Hela cells grow rapidly and are difficult to synchronize. Thus, genes involved in the control of cell cycle and growth might escape detection. Therefore, human primary cells, like human lung fibroblasts (IMR-90) or foreskin cells (HFFs) have been used for a series of studies (36-40). In these cells adenovirus DNA replication starts 24 hours post infection (hpi). Based on cellular transcription profiles, an adenovirus type 2 (Ad2) infection of IMR-90 cells can be divided into four periods (36). The first period (1-12 hpi) extends from the attachment of Ad2 to the cell surface to the beginning of adenoviral early gene expression. During this time, the cellular gene expression changes are mainly triggered by the virus entry process, including attachment of the virus to cell surface receptors, and intracellular transport of the virus along microtubules. The majority of the genes deregulated during the first phase have functions linked to inhibition of cell growth and immune response. The second period covers the time from the expression of the immediate early E1A gene to the time when Ad2 DNA replication starts (12-24 hpi). During this period, there is a linear increase in the number of differentially expressed cellular genes involved primarily in cell cycle regulation and cell proliferation. The third period ranges from the beginning of DNA replication to the time when the cytopathic effect (CPE) starts (24-36 hpi). By this time, the virus has gained control of the cellular metabolic machinery, resulting in an efficient replication of the viral genome and expression of the capsid proteins. Additional changes in cellular gene expression are modest during this phase. The final period starts when CPE is apparent (after 36 hpi). The number of down-regulated genes increases

dramatically and include many genes involved in intra- and extracellular structure, leading to an efficient burst of progeny.

The transcriptomics and proteomics of host cell during human adenovirus infection have been extensively studied (39-43). Early studies of cellular genes expression in adenovirus subtype C infected quiescent fibroblasts using microarray showed that genes involved in the control of cell cycle, proliferation, and growth were most highly up-regulated, while genes implicate in immune response were most significant among down-regulated genes during the early phase of infection (36, 40). With the development of high throughput sequencing technologies, the transcriptome can be explored on a genome-wide scale at single base pair resolution. A large number of differentially expressed cellular genes have been identified, and they are classified into similar gene ontology categories as identified by microarray (42). Binding sites for E2F, ATF/CREB and AP2 are prevalent in the up-regulated genes while SRF and NFkB are most dominant among down-regulated genes at two time points (12 and 24 hpi) as described in a previous study (42). Meanwhile, several proteomics approaches have been applied. Improve shotgun/bottom-up liquid chromatography-tandem mass spectrometry (LC-MS/MS)-based protein detection and quantitative techniques such as Stable Isotope Labelling of Amino acids in Cell culture (SILAC) have greatly facilitated protein identification (44, 45). These technologies have been used in studies of protein expression in an adenovirus-infected cells. Lam et al have analyzed the nucleolar proteome in Ad5-infected Hela cells (46) while Evans et al have examined the posttranscriptional stability of cellular protein in Ad5-infected Hela cells (41). Recently, a comparative proteome analysis of wild type and E1B-55K was performed to investigate the role of Ad5 E1B-55K in targeting cellular proteins with antiviral activity for proteasomal degradation (47). Furthermore, using a combined immunoaffinity purification and LC-MS protocol, a set of 92 E1B-associated proteins were identified in Ad5-infected HFFs and it was shown that these proteins are

enriched for function in the ubiquitin-proteasome system, RNA metabolism and cell cycle (48). Previously, we have presented a comparison of the cellular transcriptome and proteome of Ad2-infected IMR-90 cell at 24 and 36 hpi (39). More than 700 proteins were identified to be differentially expressed. Surprisingly, there was a very low correlation between the RNA and protein expression profiles. Here, we present a more comprehensive study of the cellular transcription profiles at four critical stages of an adenovirus infection in normal cell using paired-end sequencing. As a step further, RNA expression profiles were compared with protein expression profiles with a focus on genes involved in the cellular immune response.

Materials and methods

Cell culture and virus infection

Human primary lung fibroblast IMR-90 cells (American Type Culture Collection, ATCC) were initially cultured in Eagle's minimum essential medium (EMEM) (ATCC) supplemented with 10% fetal bovine serum (FCS), 100 U/ml penicillin and 100 µg/ml streptomycin at 37 °C and 5% CO_2. Cells were maintained in the plates for two days before infection. By fluorescence-activated cell sorting (FACS) analysis, more than 95% of the cells were characterized in G0/G1 phase. Synchronized cells were then infected with human adenovirus type 2 at a multiplicity of infection (MOI) of 100 fluorescence-forming units (FFU) in serum-free medium. Mock-infected cells were used as a control. One hour later, the medium was replaced with complete EMEM medium supplemented with 10% FBS. Infected cells were harvested and collected at 6, 12, 24, and 36 hours post infection (hpi).

Total RNA extraction, RNA library construction and sequencing

Total RNA from infected IMR-90 cells were extracted with TRIzol® (Invitrogen), according to the manufacturer's instructions. The quality of total RNA was evaluated with a NanoDrop 1000 spectrophotometer and an Agilent 2100 Bioanalyzer. After treatment with Ribo-Zero™ rRNA removal reagent, total RNA was used to construct cDNA library for transcriptome sequencing following the ScriptSeq™ v2 RNA-Seq library preparation kit according to the manufacturer's protocol (Epicentre). The cDNA libraries were sequenced on a HiSeq 2000 sequencing platform (Illumina).

Genome alignment and gene expression profile

Data cleaning was performed by removing low quality, contaminant and adapter reads from the raw reads. TopHat2 and Cufflinks were used to align the filtered reads to human Ensembl genome (http://www.ensembl.org/index.html, GRCh38) and to profile gene

expression following the protocol (49), respectively. FPKM (fragments per kilobase of exon per million fragments mapped) method was employed to normalize gene expression. To strengthen the reliability of our results, lowly expressed genes (< 10 FPKM in all libraries) were filtered out.

Identification of differentially expressed genes in Ad2-infected cells

To identify genes deregulated in early and late phases of Ad2 infection, we performed correlation analysis between samples based on normalized gene expression values using the CORREL function provided by Excel. To identify differentially expressed genes in the cells infected by Ad2, several statistical values were used. First, a fold change of a particular gene in Ad2-infected cells was calculated following the rule: fold change (Ad2-infected/mock) =y/x, while y and x represent the normalized expression values in Ad2-infected and mock cells, respectively. A cut-off of more than 2-fold increase or decreas was used. Second, a p-value that represents the significance for differential expression was calculated based on Poison distribution (50). A cut-off for p-values (< 0.05) was used for differentially expressed genes. Last, an R package called NOISeq was used to calculate the probability of differential expression of a gene in a comparison (51). Only those genes with probability > 0.7 were kept for further analysis.

Gene Ontology and KEGG pathway enrichment

To determine the biological processes and KEGG pathways affected by human adenovirus type 2, differentially expressed genes were analyzed by DAVID Bioinformatics Resources 6.7 (http://david.abcc.ncifcrf.gov/) (52).

SILAC-MS experiment and protein identification

The IMR-90 cells culture and protein labelling were performed as described before (36). Briefly, after growing in cell culture medium containing with heavy or light amino acids for at

least six passages, cells were mock infected or infected with Ad2 at MOI of 100 FFU per cell in serum-free medium (53). A biological replicate with swapped labeling was also performed. After harvest, cells were lysed and mock- and Ad2-infected lysates of different labeling were combined in a 1:1 protein ratio. Proteins were fractionated using SDS-PAGE. Following in-gel tryptic digestion (54), peptides were extracted and analyzed using nano liquid chromatography coupled on-line to a QExactive Orbitrap Plus Mass spectrometer (ThermoFisher Scientific, Bremen,Germany). Acquired data (raw-files) were imported into MaxQuant software (version:1.4.5.7) (55), and searched against a FASTA-file containing both cellular and Ad2 proteins downloaded from UniProt 2017-02. The ratio of the chromatographic areas of heavy and light peptides matching to specific proteins was used for determining the protein expression levels.

Results and discussion

Host cell transcriptional profiles during the course of an adenovirus infection

Alternation of cellular transcription in adenovirus infected cells has been studied before using RNA sequencing (36). However, this study included only two time points (12 and 24 hpi) in lung fibrobalst using constrained 76 bp long sequencing reads. Therefore, a more detailed study of transcription at different phases of infection using a up-graded sequencing technique is recalled. Furthermore, the correlation between transcription and protein expression need to be adressed. To this end, we have applied paired-end sequencing technology to examine the cellular RNA expression profile at 6, 12, 24 and 36 hours post infection (hpi) of IMR-90 cells. These time points represent different stages of Ad2 infection and all of our early studies on cellular various RNA expression including micro RNA (miRNA), long non-coding (lncRNA) and protein were performed under the same condition (36-38). Thus, we could correlated the expression profile between them. About 30 million 255 bp long sequence reads per sample were generated and 53-58% of them accounted for mRNA. From them 6,860 cellular genes were identified to be transcribed to a significant level with a minimum of 10 FPKM (fragments per kilobase of exon per million fragments mapped) (Table 1). Among them, 3556 genes were changed more than or equal to 2-fold with p-values<0.05 in infected cells as compared to non-infected cell. This selection of differentially expressed genes is strict. Very limited changes in RNA expression occurs during the early phases. Only 74 and 223 genes showed significant differential expression at 6 and 12 hpi, respectively. Most expression changes took place at 24 hpi when infection proceeded into the late phase, 2239 and 3060 genes were differentially expressed at 24 and 36 hpi, respectively. Fewer differentially expressed genes were detected in this study as compared to our early study, in which 1267 and 3683 cellular genes were selected as differentially expressed at 12 and 24 hpi.

241 However, the former study was less stringent and included gene covered with more than 1
242 reads (42).

243 Based on the kinetics of changes of gene expression at different stages of infection,
244 3451 out of 3556 genes fell into 20 major different expression clusters (Figure 1). The
245 complete list of genes in each cluster is included in supplementary Table S1. At 6 hpi, more
246 than 87% of the differentially expressed genes were up-regulated (cluster 1+2+3+4).
247 Expression of nearly all of these genes reached their highest level at 6 hpi, except two which
248 reached their highest levels at 12 hpi. Then about 80% of them became down-regulated during
249 the late phase of infection (clusters 1 and cluster 2). The rest either remained up-regulated
250 (cluster 4), or were gradually reduced to the basal level in the late phase (cluster 3). Only 9
251 genes (cluster 5) were down-regulated at 6 hpi and their expression remained suppressed until
252 the late phase.

253 At 12 hpi, 122 and 78 genes, became up- and down-regulated in addition to the
254 differentially expressed genes at 6 hpi. Among the up-regulated genes, about 1/3 increased
255 until 36 hpi (Cluster 6), 1/3 remained at a similar level through the rest of the infection
256 (cluster 7), and the remaining 1/3 was only transiently up-regulated at 12 hpi (Cluster 9) and
257 became down-regulated at 24 hpi (cluster 11) or at 36 hpi (cluster 10). Except one gene, all
258 down-regulated genes at 12 hpi remained suppressed until the late phase (cluster 12).

259 The most dramatic changes in gene expression took place between 12 to 24 hpi then
260 the infection proceeded from the early to the late phase. Thus, expression of 1585 and 447
261 (2032 in total) additional genes were up- and down-regulated at 24 hpi. Based on the
262 expression changes at 36 hpi, the up-regulated genes at 24 hpi fell into four profiles (Cluster
263 13+14+15+16). Expression of 59% of these genes increased until 36 hpi (Cluster 13), whereas
264 25% decreased but remained higher (>2-fold) than in non-infected cells (Cluster 14) and 15%
265 declined to less than 2-fold change at 36 hpi (Cluster 15). Only 6 genes became down-

regulated at 36 hpi (Cluster 16). Among 447 down-regulated genes, 75% decreased continually until 36 hpi (Cluster 17), while 25% remained at a similar level (Cluster 18). Change in cellular gene expression was modest between 24 to 36 hpi as compared to that between 12 to 24 hpi. In comparison to non-infected cells, expression of 737 (Cluster 19) and 408 genes (Cluster 20) became up- or down-regulated at 36 hpi in addition to the genes that were differentially expressed at 12 or 24 hpi.

Biological functions of genes in different expression clusters

The biological consequences of the gene expression changes were analyzed using DAVID (The Database for Annotation, Visualization and Integrated Discovery) and are shown in Figure 1 (left hand panel), and more detailed results are included in supplementary Table S1. The most significant functions of the genes that were transiently up-regulated at 6 hpi (clusters 1-3) were cellular proliferation, antiviral response and cellular signaling. A significant group of genes was cytokines involved stress/immune response and cell growth control. Genes implicated in apoptosis and cell cycle control were also noteworthy. Among transcription factors, up-regulation of ATF3 was the most significant since it reached 6-fold compared to the non-infected control. Expression of ATF3 has been shown to be induced by a variety of signals and is involved in cellular stress response. Only 9 genes were present in cluster 5 and therefore no significant functional categories could be identified by DAVID. However, four (PTPN12, MAP4K3, ERRFI1 and LBH) out of the 9 genes, are involved in cellular signaling and growth control.

During the period between 6 and 12 hpi, adenovirus early genes begin to be expressed, redirecting cellular gene expression. The up-regulated cellular genes are involved in DNA replication (Clusters 6 and 7), including Minichromosome Maintenance Complex Components (MCM) 3, 4, 5, 6, 7 and components of the post-replicative DNA mismatch

repair system (MMR) alpha (MSH2-MSH6 heterodimer). In addition, genes implicate in transcription and pre-RNA processing were prominent in cluster 6. Genes implicated in cell cycle were significant in Cluster 7, including CDC25A, CCNE2, CCNE1 and CDK2, the key regulators for the progression from G1 to the S phase. Although no significant function was identified for clusters 8 to 11, several genes, such as JunB, GADD45B and PAPPA function in control of cell growth and proliferation were included in this cluster. The most significant function for the down-regulated genes was actin cytoskeleton organization.

There was a dramatic increase in the number of differentially expressed genes between 12-24 hpi. Cellular genes which function in protein translation became significant among up-regulated genes. These genes covered both cytoplasmic and mitochondrial ribosomal proteins (RPLs/RPSs and MRPLs/MRPSs), eukaryotic translation initiation factors (EIFs), and eukaryotic translation elongation factors (EEFs). Although genes involved in DNA replication and cell cycle were still significant, similar to those at 12 hpi, the number of genes in these categories increased dramatically. For instance, genes involved in DNA metabolism/DNA replication increased from 18 to 124, whereas genes implicated in cell cycle increased from 19 to 153. Most of these genes were included in clusters 13, 14 and 15. The genes involved in DNA replication included DNA polymerases, replication factor C (RFC) and histones from all five families. The large number of genes involved in the cell cycle included many key regulators, such as E2Fs, cyclins, cyclin dependent kinases and cell division cycle (cdc) genes. In addition, genes participating in RNA processing became significant, comprising RNA helicases, the splicing factors, U2 small nuclear RNA auxiliary factors, U3 small nucleolar ribonucleoprotein, U6 small nuclear RNA associated, pre-mRNA processing factors (PRPFs), heterogeneous nuclear ribonucleoproteins (HNRNPs) and small nuclear ribonucleoproteins (SNRNPs). Furthermore, the THO complexes 3, required for efficient export of polyadenylated RNA, were up-regulated, as were the cleavage and polyadenylation

specificity factors (CPSFs), playing a key role in the 3' end cleavage of pre-mRNAs and polyadenylation. Several important components of the exosome complex involved in the degradation and processing of a wide variety of RNA species were also up-regulated.

The number of down-regulated genes between 12 and 24 hpi also increased (clusters 17 and 18). The most significant function of these clusters were cellular signaling, such as TGFBR1, TGFBR2, BMPR2, ACVR1 and SMAD3 involved in TGFβ signaling, as well as growth factors, like EGFR, DGFRA, HBEGF, PDGFC, PLAT, TXNIP, ZFAND5, ARID5B, BCAR1, PDGFRA, PDGFC, VEGFC, NRP1 and PDGFRB. Cytoskeleton organization was significant for genes in cluster 17, whereas genes implicated in cell adhesion were significant in cluster 18.

Previous experiments have shown that the replication of Ad2 DNA reaches a maximum rate during the period from 24 to 36 hpi (36). However, cellular gene expression was still maintained at a high level. The most significant function of the up-regulated genes (cluster 19) was protein translation similar to that at 24 hpi, but with an increased number of genes. Genes involved in the generation of precursor metabolites and energy, as well as oxidation reduction became significant. In addition, several genes identified in different diseases were also significant. The major function for the down-regulated genes (cluster 20) was cellular macromolecule catabolic processes such as ubiquitination and subsequent proteasomal degradation of target proteins. Another significant function was small GTPase mediated signal transduction, involved in vesicle transport.

Consensus transcription factor binding sites in the promoter region of genes in the different clusters

Genes sharing a similar transcription profile are likely to be regulated by the common transcription factors (TF) or TFs from the same family. To this end, the genes in the 20

different clusters were subjected to analysis for the presence of consensus TF binding sites in their promoter regions (-300 to +100) using Transfind (56). The top ten of the over-represented TF binding sites are listed in the order of significance and are included in the supplementary Table S2. NFκB and c-Rel binding sites were most significant for the genes in cluster 1. Interesting genes among them were BIRC3, IKBA, IL8, CCL20, GROA (CXCL1), TNAP3 and TNF15. These genes are known to be involved in immune response or apoptosis. No significant enrichment of TF binding sites was identified for the genes in clusters 2, 3, 4, 5. For the genes in clusters 6 and 7, only the E2F binding site was significant. Genes with E2F binding sites became more significant in clusters 13, 14 and 19. In addition, the binding sites for GABP, NRF1, and ATF/CREB family were significant among genes in clusters 13, 14 and 15. GABP regulates genes that are involved in cell cycle control, protein synthesis, and cellular metabolism. NRF1 activates the expression of key metabolic genes regulating cellular growth. The ATF/CREB family has diverse functions in controlling cell proliferation and apoptosis. In contrast, the TF binding sites among the down-regulated genes were less significant. Only the MZF1 and AP2 binding sites were scored but their significance was low and they were only present on 8 or 7 genes, respectively. MZF1 can function as a tumor/growth suppressor and controls cell proliferation and tumorigenesis (57). At 36 hpi, different sets of TF binding sites became significant for up-regulated genes (cluster 19), including SP1, STRA13 and NF-Y in addition to GABP while the binding sites for E2F became less significant. This correlated very well with the expression profile of E2Fs. Expression of all E2Fs increased at 12 and 24 hpi, and then decreased at 36 hpi. The TF binding sites for the down-regulated genes were less significant and STRA13 and USF were on the top of the list. STRA13 is a transcriptional repressor. Correspondly, its expression increased 4 and 8 times at 24 and 36 hpi, respectively. STRA13 is involved in DNA damage repair and genome maintenance. Surprisingly, the STRA13 binding site was significant for

both up- and down-regulated genes at 36 hpi. Its transcriptional repression is probably mediated by recruitment of other regulatory factors and, depending on the cofactors, STRA13 plays divergent roles. USF that binds to a symmetrical DNA sequence (E-boxes; 5-CACGTG-3) is involved in the transcriptional activation of various genes implicated in physiological processes, such as stress response, immune response, cell cycle control and tumor growth.

Inconsistency between changes in RNA and protein expression highlighted in genes involved the cellular immune signaling pathway

About 35% of genes that were expressed at the RNA level here were detected at the protein level at 24 and 36 hpi as shown in our previous study using high throughput SILAC-MS technology (Zhao et al 2017). Among 2648 and 2394 proteins that were detected at 24 and 36 hpi, expression of 659 and 645 protein were changed ≥ 1.6-fold as compared to the uninfected control. The correlation between changes in RNA and protein expression was surprisingly low (r=0.3). The functions of the discordantly expressed proteins were analyzed using the web-based tool DAVID, a functional enrichment analysis by intergrating a wide-range heterogeneous data content. However, this tool is less specific for analysis data of virus-induced changes in gene expression because of under representive of genes related to virus infection. In addition, our previous analysis included only proteins that had minimum fold-change of 1.6 and proteins with a slow kinetic of synthesis or degradation might have escaped detection. Nonetheless, we noted that several genes which showed opposite profiles for RNA and protein expression were involved in immune response. Here, we have extended our comparison between RNA and protein expression on genes involved in cellular immune pathways including new SILAC-MS data for 6 and 12 hpi (manuscript submitted for publication). Significantly, many key regulators in cellular immune pathways, NFκB, STAT, apoptosis and MAV displayed inconsistent expression profiles between RNA and protein expression as listed Table 2 and their expression profiles are shown in Figure 2.

As presented above, NFκB and c-Rel binding sites were the most significant in the promoter region of genes that were transiently up-regulated during the early phase. Indeed, expression of several key factors of the NFκB pathway were significantly changed at both the RNA and protein levels (Figure 2A). The transcription of all NFκB family members was detectable, and NFκB1 was the most highly expressed. Except REL, all showed very similar expression profiles. Specifically, they were moderately induced during the early phase, but decreased rapidly and became down-regulated after 24 hpi. Among them, expression of RELA, NFκB1 and NFκB2 was also detectable at the protein level. Coupled with the increased RNA level at 6 hpi, these proteins were all up-regulated. Unexpectedly the NFκB2 and RELA protein levels remained constant until the late phase of infection in spite of the reduction in transcription. The members of NFκB inhibitor family (IκB) displayed diverse transcription profiles. NFKBIA (IκBα) and NFKBIZ (IkBζ) were the most highly expressed and showed similar expression profiles, transiently up-regulated at 6 hpi but decreased at12 hpi and were reduced more than 8-fold at 36 hpi. NFκBIB (IκBβ) showed an opposite expression pattern, low in uninfected cells and at 6 hpi, but increased after 12 hpi and became up-regulated more than 16-fold at 36 hpi. Thus, it appears that NFKBIB replaced NFKBIA to be the most highly expressed IκB in the late phase. None of these gene products was detected at the protein level. The expression changes of the inhibitors of NFκB kinases (IKKs) subunit, IKBKB, and its regulatory subunit IKBKG, as well as IKK-related kinases, IKBKE and TBK1, appeared to be coordinated. They were delayed as compared to the expression of NFκBs and IκBs and significant down-regulation of transcription occurred at 24 or 36 hpi. A surprising finding was that the expression of IKBKB and TBK1 was up-regulated at the proteins level. The IKBKB protein was up-regulated already at 6 hpi and remained stable until the late phase while the up-regulation of the TBK1 protein was significant after 24 hpi. The

results thus indicate that the positive regulators of the NFκB pathway are activated at both the RNA and protein levels during the early phase of infection as result of the host immediate response to the infection. Following the progression of the infection, these proteins remained up-regulated until 36 hpi although their transcription was suppressed. However, the fact that the downstream target genes of the NFκB pathway were down-regulated during the late phase indicates that these proteins have lost their functions as transcriptional activitors. The dramatic up-regulation of NFKIB may contribute to the inhibition of the NFκB activity. Other post-translational control mechanisms, such as the blocking of the nuclear transport, loss of its coactivator such as CBP/P300, p400 and TRAPP due to interaction with the Ad2 E1A protein, may contribute to the block of the NFκB activity (58, 59). Other yet unidentified mechanism might also cause the inactivation of the NFκF pathway.

The Janus kinase-signal transducer and activator of transcription (JAK/STAT) signaling is another important pathway regulating the innate immune response. Transcription of all STATs (STAT1, STAT2, STAT3, STAT5A/B and STAT6) was unchanged up to 12 hpi, but were then down-regulated after 24 hpi. Four STAT proteins (STAT1, STAT2, STAT3 and STAT6) were detected and they were up-regulated during the early phase and remained stable or decreased slightly in the late phase. JAKs are important activators of STAT and catalyse the phosphorylation of the STAT proteins. The three JAK kinases, JAK1, JAK2 and TYK2, displayed different expression profiles. JAK1 was the most highly transcribed and only slightly increased at 6 hpi. Then, it decreased to the basic level and remained constant until the late phase. Transcription of both JAK2 and TYK2 increased at 12 hpi. JAK2 decreased during the late phase while TYK2 remained constant. Only JAK1 protein was detected and it decreased slightly during the early phase, but became up-regulated at 24 hpi. The activity of the STAT proteins is also controlled by several negative regulators, including protein tyrosine phosphatase (PTPN), suppressor of cytokine signaling (SOCS) and protein inhibitor of

activated STAT (PIAS). Several PTPNs were detected at both RNA and protein levels with inconsistent expression profiles. Either their RNAs were down-regulated, while their protein levels remained constant (PTPN1) or increased (PTPN12). In other cases the RNA remained stable, while the protein level was increased (PTPN11). Furthermore, several Importins and Ran, required for nuclear translocation of STATs, were up-regulated at both at the RNA and protein levels during the infection. Suppression of STAT transcription and promotion of STAT translation during Ad2 infection might reflect an aspect of the battle between the virus and its host. Through several distinct routes the infected cells recognize different viral components and active the expression of IFNβ which leads the stimulation of the JAK/STAT pathway. In turn, viruses have developed strategies to circumvent the IFNβ response (60). Expression of most, if not all, of the downstream targets of the STAT pathway were suppressed, indicating that the STAT pathway is blocked (data not shown). Apparently, the inhibition of the STAT pathway occurs both transcriptional and post-translationally. The activity of STATs has been shown to be modulated by various posttranslational modifications (61, 62). Upon infection, adenovirus uses several strategies to block the STAT pathway. The viral E1A plays a significant role in the inactivation of the STAT pathway by binding to STATs, or their coactivator CBP/p300.(11, 63-65). Meanwhile, the E1B-55k protein represses expression of IFN-inducible genes which leads to the inhibition of the STAT signaling pathway (66). In addition, E3-14.7K protein interacts with STAT1 which results in the inhibition of STAT1 phosphorylation and nuclear translocation (67). Furthermore, phosphorylated STAT1 has been shown to be sequestered at viral replication centers in the nuclues (68).

Apoptosis pathways are extensively regulated during Ad2 infection. Our RNA sequencing results showed that transcription of more than 60% of genes that are directly involved in apoptosis were down-regulated, whereas only 20% were up-regulated in the late

phase (data not shown). Transcription of most TNF family ligands was undetectable or at a very low level except for TNFSF15 and TNFSF4 (Table 2). Both of them decreased after 12 hpi, although TNFSF15 was transiently induced more than 6-fold at 6 hpi. Numerous TNF receptor superfamily members were expressed at the transcriptional level with diverse expression profiles. TNFRSF11B and TNFRSF12A were the most highly expressed receptors. After being slightly increased at 6 hpi, their RNA levels decreased at 12 hpi and were then more than 25- and 6-fold lower at 36 hpi as compared to the non-infected control. Unfortunately, none of the TNF receptor superfamily members was detected at the protein level.

Caspases (CASPs) and the Bcl2 families are key player in apoptosis. At the transcriptional level, CASPs showed different expression profiles. Among them, CASP1, 3 and 4 are most highly expressed with similar expression profiles, slightly increased at 6 hpi and then down-regulated. All of these CASPs were detected at the protein level and were up-regulated, opposite to their RNA expression profile. Expressions of most Bcl2 family members were low at the RNA level except for those listed in the Table 2. Transcriptions of most anti-apoptotic BCLs (BCl2A1, BCL2L1, BCL2L13 and MCL1) were down-regulated after a slight increase at 6 hpi. Among them, only BCL2L13 protein was detected which showed 40% increased expression during the late phase. Among pro-apoptotic genes, transcription of BID, BAD and BAX was up-regulated gradually towards the late phase or remained stable. At the protein level, BID and BAX were up-regulated from the early to the late phase, although the RNA level for BAX decreased in the late phase. BAD protein displayed an expression pattern opposite to its RNA.

Although most genes that are directly involved in apoptosis were down-regulated at the transcriptional level, several important pro-apoptotic players were up-regulated at the protein level (CASP3, BAX and BID). The fact that apoptosis is efficiently inhibited during an

adenovirus infection indicated that the functions of these proteins must be inactivated. To counteract the host defensive apoptotic pathways, adenoviruses have established very efficient mechanisms by encoding their own anti-apoptotic proteins in the E1B and E3 regions. Obviously, the regulation of apoptosis is very multifaceted and a comprehensive view of how apoptosis is blocked during an Ad2 infection remains to be unraveled.

Inconsistent expression profiles between RNA and protein for the genes involved in MAVS was shown in our previous study (39). We show here that expression of MAVS is stable at both RNA and protein levels during the early phase, whereas difference were seen in the late phase. In addition, we have studied the expression of three MAVS regulatory proteins, PSMA7, PCBP2 and TBK1. The expression profiles of the negative regulators PSMA7 and PCBP2 were similar at both the RNA and protein levels, and increased slowly during infection. The positive regulator, TBK1 showed an opposite profile; its RNA was down-regulated at 36 hpi whereas its protein level increased after 24 hpi. In spite of the up-regulation of MAVS and its positive regulator, expression of its target genes (type I interferon genes) was very low or undetectable, suggesting that this antivirus pathway is inactivated during the late phase.

Furthermore, different expression profiles were also observed for galectins LGALS. LGALS3 and 8 (Gal3 and 8) were the most highly expressed among LGALSs and their RNAs were down-regulated after 24 hpi. However, their proteins remained constant from early to late phase. Galectins have been shown to involve in innate immune processes (69). Colocalization of LGALS3 with incoming Ad5 has been observed and its role in Ad5 transport was suggested (70). Stable expression of LGALS3 has been reported previously in Ad5-infected cells, while it is down-regulated in Ad3-infected cells (71).

Apparently, there are features common to genes which participate in important immune pathways, being suppressed at the transcriptional level while being enhanced or

513 stable at the protein level during the late phase. Thus, we hypothesize that the transcriptional
514 regulation of these genes is mediated mainly by Ad2, while protein translation machinery is
515 not yet completely under the control of the virus. The increased protein expression could be
516 caused by increased translation and/or decreased protein degradation. The facts that most of
517 downstream genes of immune pathways are down-regulated at RNA level in the late phase
518 even though their key regulators are stable or up-regulated at the protein level. Apparently,
519 adenovirus-mediated post-translational mechanisms play a very important role. As discussed
520 above, inhibition of STAT pathway represent the best example how adenovirus has evolved
521 redundant strategies to counteract cellular immune response. By regulating protein
522 modification, blocking of protein-protein interactions, inhibiting of the protein transport to its
523 destination, or direct interacting, adenovirus controls host cell antiviral pathways. Last but not
524 least, non-coding RNAs (ncRNAs) have been shown to be important regulators of various
525 biological processes. Alternations of cellular miRNA and lncRNA expression during Ad2
526 infection have been studied using RNA-seq (37, 38). Significant changes in their expression
527 take place after 24 hpi. The strong correlation of ncRNA expression changes with infection
528 progression indicates that ncRNA play important roles during infection. Specially, majority of
529 differentially expressed miRNAs were down-regulated in the late phase. One major
530 mechanisms of miRNA in gene regulation is the suppression of translation through partial
531 complementary to 3' UTRs of mRNA. Thus, down-regulation of miRNAs could lead to stable
532 or increase translation of special sets of proteins. In contrast, most of differencially expressed
533 cellular lncRNAs were up-regulated in the late phase. Several lncRNAs that are predicted to
534 target immune response genes were down-regulated in the late phase. In addition, a large
535 share of differentially expressed lncRNA are associated with RNA-binding proteins (RBPs),
536 being involved in posttranscriptional RNA processing and translation regulation. However,

how they are regulated, and how they are involved in the regulation of cellular gene expression during adenovirus infection nees to be further addessed.

Acknowledgments

Sequencing was performed at the SNP&SEQ Technology Platform at Uppsala University and University Hospital. We thank Ulrika Liljedahl and Johanna Lagensjö for excellent sequencing. Martin Dahlö at UPPMAX is acknowledged for helping to make the code run on the UPPMAX resources. We thank Dr. Caroline Gallant for critical reading of the manuscript. This work was supported by the Kjell and Märta Beijer Foundation (UP), Åke Wiberg Foundation (SBL) and Magnus Bergvall Foundation (SBL).

References

549 1. Ferrari R, Pellegrini M, Horwitz GA, Xie W, Berk AJ, Kurdistani SK. 2008. Epigenetic
550 reprogramming by adenovirus e1a. Science 321:1086-8.
551 2. Flint J, Shenk T. 1997. Viral transactivating proteins. Annu Rev Genet 31:177-212.
552 3. Bayley ST, Mymryk JS. 1994. Adenovirus e1a proteins and transformation (review). Int J
553 Oncol 5:425-44.
554 4. Braun T, Bober E, Arnold HH. 1992. Inhibition of muscle differentiation by the adenovirus
555 E1a protein: repression of the transcriptional activating function of the HLH protein Myf-5.
556 Genes Dev 6:888-902.
557 5. Caruso M, Martelli F, Giordano A, Felsani A. 1993. Regulation of MyoD gene transcription
558 and protein function by the transforming domains of the adenovirus E1A oncoprotein.
559 Oncogene 8:267-78.
560 6. Chellappan S, Kraus VB, Kroger B, Munger K, Howley PM, Phelps WC, Nevins JR. 1992.
561 Adenovirus E1A, simian virus 40 tumor antigen, and human papillomavirus E7 protein share
562 the capacity to disrupt the interaction between transcription factor E2F and the retinoblastoma
563 gene product. Proc Natl Acad Sci U S A 89:4549-53.
564 7. Cobrinik D. 1996. Regulatory interactions among E2Fs and cell cycle control proteins. Curr
565 Top Microbiol Immunol 208:31-61.
566 8. Chakravarti D, Ogryzko V, Kao HY, Nash A, Chen H, Nakatani Y, Evans RM. 1999. A viral
567 mechanism for inhibition of p300 and PCAF acetyltransferase activity. Cell 96:393-403.
568 9. Reid JL, Bannister AJ, Zegerman P, Martinez-Balbas MA, Kouzarides T. 1998. E1A directly
569 binds and regulates the P/CAF acetyltransferase. EMBO J 17:4469-77.
570 10. Chinnadurai G. 2004. Modulation of oncogenic transformation by the human adenovirus E1A
571 C-terminal region. Curr Top Microbiol Immunol 273:139-61.
572 11. Ackrill AM, Foster GR, Laxton CD, Flavell DM, Stark GR, Kerr IM. 1991. Inhibition of the
573 cellular response to interferons by products of the adenovirus type 5 E1A oncogene. Nucleic
574 Acids Res 19:4387-93.

12. Berhane S, Areste C, Ablack JN, Ryan GB, Blackbourn DJ, Mymryk JS, Turnell AS, Steele JC, Grand RJ. 2011. Adenovirus E1A interacts directly with, and regulates the level of expression of, the immunoproteasome component MECL1. Virology 421:149-58.

13. Harada JN, Shevchenko A, Shevchenko A, Pallas DC, Berk AJ. 2002. Analysis of the adenovirus E1B-55K-anchored proteome reveals its link to ubiquitination machinery. J Virol 76:9194-206.

14. Schwartz RA, Lakdawala SS, Eshleman HD, Russell MR, Carson CT, Weitzman MD. 2008. Distinct requirements of adenovirus E1b55K protein for degradation of cellular substrates. J Virol 82:9043-55.

15. Querido E, Blanchette P, Yan Q, Kamura T, Morrison M, Boivin D, Kaelin WG, Conaway RC, Conaway JW, Branton PE. 2001. Degradation of p53 by adenovirus E4orf6 and E1B55K proteins occurs via a novel mechanism involving a Cullin-containing complex. Genes Dev 15:3104-17.

16. Farrow SN, White JH, Martinou I, Raven T, Pun KT, Grinham CJ, Martinou JC, Brown R. 1995. Cloning of a bcl-2 homologue by interaction with adenovirus E1B 19K. Nature 374:731-3.

17. Han J, Sabbatini P, Perez D, Rao L, Modha D, White E. 1996. The E1B 19K protein blocks apoptosis by interacting with and inhibiting the p53-inducible and death-promoting Bax protein. Genes Dev 10:461-77.

18. Lomonosova E, Subramanian T, Chinnadurai G. 2005. Mitochondrial localization of p53 during adenovirus infection and regulation of its activity by E1B-19K. Oncogene 24:6796-808.

19. Wold WS, Tollefson AE, Hermiston TW. 1995. E3 transcription unit of adenovirus. Curr Top Microbiol Immunol 199 (Pt 1):237-74.

20. Bennett EM, Bennink JR, Yewdell JW, Brodsky FM. 1999. Cutting edge: adenovirus E19 has two mechanisms for affecting class I MHC expression. J Immunol 162:5049-52.

21. Burgert HG, Kvist S. 1987. The E3/19K protein of adenovirus type 2 binds to the domains of histocompatibility antigens required for CTL recognition. EMBO J 6:2019-26.

603 22. Wold WS, Doronin K, Toth K, Kuppuswamy M, Lichtenstein DL, Tollefson AE. 1999.
604 Immune responses to adenoviruses: viral evasion mechanisms and their implications for the
605 clinic. Curr Opin Immunol 11:380-6.
606 23. Tollefson AE, Toth K, Doronin K, Kuppuswamy M, Doronina OA, Lichtenstein DL,
607 Hermiston TW, Smith CA, Wold WS. 2001. Inhibition of TRAIL-induced apoptosis and
608 forced internalization of TRAIL receptor 1 by adenovirus proteins. J Virol 75:8875-87.
609 24. Friedman JM, Horwitz MS. 2002. Inhibition of tumor necrosis factor alpha-induced NF-kappa
610 B activation by the adenovirus E3-10.4/14.5K complex. J Virol 76:5515-21.
611 25. Neill SD, Hemstrom C, Virtanen A, Nevins JR. 1990. An adenovirus E4 gene product trans-
612 activates E2 transcription and stimulates stable E2F binding through a direct association with
613 E2F. Proc Natl Acad Sci U S A 87:2008-12.
614 26. Obert S, O'Connor RJ, Schmid S, Hearing P. 1994. The adenovirus E4-6/7 protein
615 transactivates the E2 promoter by inducing dimerization of a heteromeric E2F complex. Mol
616 Cell Biol 14:1333-46.
617 27. Leppard KN, Everett RD. 1999. The adenovirus type 5 E1b 55K and E4 Orf3 proteins
618 associate in infected cells and affect ND10 components. J Gen Virol 80 (Pt 4):997-1008.
619 28. Kleinberger T, Shenk T. 1993. Adenovirus E4orf4 protein binds to protein phosphatase 2A,
620 and the complex down regulates E1A-enhanced junB transcription. J Virol 67:7556-60.
621 29. Chow LT, Broker TR, Lewis JB. 1979. Complex splicing patterns of RNAs from the early
622 regions of adenovirus-2. J Mol Biol 134:265-303.
623 30. Jones N. 1995. Transcriptional modulation by the adenovirus E1A gene. Curr Top Microbiol
624 Immunol 199 (Pt 3):59-80.
625 31. Cuesta R, Xi Q, Schneider RJ. 2000. Adenovirus-specific translation by displacement of
626 kinase Mnk1 from cap-initiation complex eIF4F. EMBO J 19:3465-74.
627 32. Farley DC, Brown JL, Leppard KN. 2004. Activation of the early-late switch in adenovirus
628 type 5 major late transcription unit expression by L4 gene products. J Virol 78:1782-91.

629 33. Hayes BW, Telling GC, Myat MM, Williams JF, Flint SJ. 1990. The adenovirus L4 100-
630 kilodalton protein is necessary for efficient translation of viral late mRNA species. J Virol
631 64:2732-42.
632 34. Bridge E, Ketner G. 1990. Interaction of adenoviral E4 and E1b products in late gene
633 expression. Virology 174:345-53.
634 35. Flint SJ, Gonzalez RA. 2003. Regulation of mRNA production by the adenoviral E1B 55-kDa
635 and E4 Orf6 proteins. Curr Top Microbiol Immunol 272:287-330.
636 36. Zhao H, Granberg F, Pettersson U. 2007. How adenovirus strives to control cellular gene
637 expression. Virology 363:357-75.
638 37. Zhao H, Chen M, Lind SB, Pettersson U. 2016. Distinct temporal changes in host cell lncRNA
639 expression during the course of an adenovirus infection. Virology 492:242-50.
640 38. Zhao H, Chen M, Tellgren-Roth C, Pettersson U. 2015. Fluctuating expression of microRNAs
641 in adenovirus infected cells. Virology 478:99-111.
642 39. Zhao H, Konzer A, Mi J, Chen M, Pettersson U, Lind SB. 2017. Posttranscriptional
643 Regulation in Adenovirus Infected Cells. J Proteome Res 16:872-888.
644 40. Miller DL, Myers CL, Rickards B, Coller HA, Flint SJ. 2007. Adenovirus type 5 exerts
645 genome-wide control over cellular programs governing proliferation, quiescence, and survival.
646 Genome Biol 8:R58.
647 41. Evans VC, Barker G, Heesom KJ, Fan J, Bessant C, Matthews DA. 2012. De novo derivation
648 of proteomes from transcriptomes for transcript and protein identification. Nat Methods
649 9:1207-11.
650 42. Zhao H, Dahlo M, Isaksson A, Syvanen AC, Pettersson U. 2012. The transcriptome of the
651 adenovirus infected cell. Virology 424:115-28.
652 43. Ying B, Toth K, Spencer JF, Aurora R, Wold WS. 2015. Transcriptome sequencing and
653 development of an expression microarray platform for liver infection in adenovirus type 5-
654 infected Syrian golden hamsters. Virology 485:305-12.
655 44. Yates JR, Ruse CI, Nakorchevsky A. 2009. Proteomics by mass spectrometry: approaches,
656 advances, and applications. Annu Rev Biomed Eng 11:49-79.

45. Ong SE, Mann M. 2006. A practical recipe for stable isotope labeling by amino acids in cell culture (SILAC). Nat Protoc 1:2650-60.

46. Lam YW, Evans VC, Heesom KJ, Lamond AI, Matthews DA. 2010. Proteomics analysis of the nucleolus in adenovirus-infected cells. Mol Cell Proteomics 9:117-30.

47. Fu YR, Turnell AS, Davis S, Heesom KJ, Evans VC, Matthews DA. 2017. Comparison of protein expression during wild-type, and E1B-55k-deletion, adenovirus infection using quantitative time-course proteomics. J Gen Virol 98:1377-1388.

48. Hung G, Flint SJ. 2017. Normal human cell proteins that interact with the adenovirus type 5 E1B 55kDa protein. Virology 504:12-24.

49. Trapnell C, Roberts A, Goff L, Pertea G, Kim D, Kelley DR, Pimentel H, Salzberg SL, Rinn JL, Pachter L. 2012. Differential gene and transcript expression analysis of RNA-seq experiments with TopHat and Cufflinks. Nat Protoc 7:562-78.

50. Audic S, Claverie JM. 1997. The significance of digital gene expression profiles. Genome Res 7:986-95.

51. Tarazona S, Garcia-Alcalde F, Dopazo J, Ferrer A, Conesa A. 2011. Differential expression in RNA-seq: a matter of depth. Genome Res 21:2213-23.

52. Huang da W, Sherman BT, Lempicki RA. 2009. Systematic and integrative analysis of large gene lists using DAVID bioinformatics resources. Nat Protoc 4:44-57.

53. Philipson L. 1961. Adenovirus assay by the fluorescent cellcounting procedure. Virology 15:263-268.

54. Shevchenko A, Chernushevich I, Wilm M, Mann M. 2000. De Novo peptide sequencing by nanoelectrospray tandem mass spectrometry using triple quadrupole and quadrupole/time-of-flight instruments. Methods Mol Biol 146:1-16.

55. Cox J, Matic I, Hilger M, Nagaraj N, Selbach M, Olsen JV, Mann M. 2009. A practical guide to the MaxQuant computational platform for SILAC-based quantitative proteomics. Nat Protoc 4:698-705.

56. Kielbasa SM, Klein H, Roider HG, Vingron M, Bluthgen N. 2010. TransFind--predicting transcriptional regulators for gene sets. Nucleic Acids Res 38:W275-80.

685 57. Gaboli M, Kotsi PA, Gurrieri C, Cattoretti G, Ronchetti S, Cordon-Cardo C, Broxmeyer HE,
686 Hromas R, Pandolfi PP. 2001. Mzf1 controls cell proliferation and tumorigenesis. Genes Dev
687 15:1625-30.
688 58. Frisch SM, Mymryk JS. 2002. Adenovirus-5 E1A: paradox and paradigm. Nat Rev Mol Cell
689 Biol 3:441-52.
690 59. Lang SE, Hearing P. 2003. The adenovirus E1A oncoprotein recruits the cellular
691 TRRAP/GCN5 histone acetyltransferase complex. Oncogene 22:2836-41.
692 60. Randall RE, Goodbourn S. 2008. Interferons and viruses: an interplay between induction,
693 signalling, antiviral responses and virus countermeasures. J Gen Virol 89:1-47.
694 61. Kim TK, Maniatis T. 1996. Regulation of interferon-gamma-activated STAT1 by the
695 ubiquitin-proteasome pathway. Science 273:1717-9.
696 62. Wen Z, Zhong Z, Darnell JE, Jr. 1995. Maximal activation of transcription by Stat1 and Stat3
697 requires both tyrosine and serine phosphorylation. Cell 82:241-50.
698 63. Bhattacharya S, Eckner R, Grossman S, Oldread E, Arany Z, D'Andrea A, Livingston DM.
699 1996. Cooperation of Stat2 and p300/CBP in signalling induced by interferon-alpha. Nature
700 383:344-7.
701 64. Kalvakolanu DV, Bandyopadhyay SK, Harter ML, Sen GC. 1991. Inhibition of interferon-
702 inducible gene expression by adenovirus E1A proteins: block in transcriptional complex
703 formation. Proc Natl Acad Sci U S A 88:7459-63.
704 65. Leonard GT, Sen GC. 1996. Effects of adenovirus E1A protein on interferon-signaling.
705 Virology 224:25-33.
706 66. Chahal JS, Gallagher C, DeHart CJ, Flint SJ. 2013. The repression domain of the E1B 55-
707 kilodalton protein participates in countering interferon-induced inhibition of adenovirus
708 replication. J Virol 87:4432-44.
709 67. Spurrell E, Gangeswaran R, Wang P, Cao F, Gao D, Feng B, Wold W, Tollefson A, Lemoine
710 NR, Wang Y. 2014. STAT1 interaction with E3-14.7K in monocytes affects the efficacy of
711 oncolytic adenovirus. J Virol 88:2291-300.

712 68. Sohn SY, Hearing P. 2011. Adenovirus sequesters phosphorylated STAT1 at viral replication
713 centers and inhibits STAT dephosphorylation. J Virol 85:7555-62.
714 69. Rabinovich GA, Toscano MA. 2009. Turning 'sweet' on immunity: galectin-glycan
715 interactions in immune tolerance and inflammation. Nat Rev Immunol 9:338-52.
716 70. Maier O, Marvin SA, Wodrich H, Campbell EM, Wiethoff CM. 2012. Spatiotemporal
717 dynamics of adenovirus membrane rupture and endosomal escape. J Virol 86:10821-8.
718 71. Trinh HV, Grossmann J, Gehrig P, Roschitzki B, Schlapbach R, Greber UF, Hemmi S. 2013.
719 iTRAQ-Based and Label-Free Proteomics Approaches for Studies of Human Adenovirus
720 Infections. Int J Proteomics 2013:581862.

721

722

723 Figure legends

724 Figure 1. Based on the kinetics of transcription changes, the differentially expressed genes were
725 grouped into 20 clusters (C1-C20). The numbers of genes in each cluster and the number of
726 differentially expressed genes identified at each time point were indicated on the right hand side (Note
727 that the numbers of genes at 12, 24 and 36 hpi are different to the Table 1 because many genes were
728 identified as differentially expressed at more than one time point, but included only in one cluster).
729 The biological functions of genes in each cluster were analyzed using DAVID (left). Red, green and
730 white arrow bars represent RNAs that were up-, down-regulated or unchanged in Ad2-infected cells in
731 comparison to RNA in uninfected control.

732 Figure 2. Schematic representation of key components of NF□B (A), STAT (B), apoptosis (C) and
733 MAVS (D) pathways. The involvement of Ad2 proteins is also indicated. Graphs display the
734 expression profiles (fold change between Ad2 and mock) of genes that detected at both protein (dash
735 line) and RNA (solid line) levels at 4 time points. The same color is used for the corresponding protein
736 and RNA.

Table 1. In total 12,927 cellular mRNAs were detected in five time points together. Among them 9,738 mRNAs were common between all time points. Expression of 6,860 mRNAs reached to a significant level with a minimum of 10 FPKM. Among them 3556 genes expressions were changed ≥2-fold in infected cells as compared to non-infected cells. Numbers of mRNAs at each time point are listed here.

Selection	**Mock**	**Ad2-6 hpi**	**Ad2-12 hpi**	**Ad2-24 hpi**	**Ad2-36 hpi**
≥ 1 FPKM	11064	11163	11837	11426	11191
≥ 10 FPKM	5001	4846	5184	4692	4371
≥ 2-Fold change		74[a]	223	2239	3060
Up-regulated		65[b]	138	1694	2142
Down-regulated		9[c]	85	545	918

[a]Number of genes expression with or decrease in Ad2-infected as compared to uninfected cells as measured by sequence reads.

[b]Number of genes expression with more than 2-fold increase in Ad2-infected as compared to uninfected cells.

[c]Number of genes expression with more than 2-fold decrease in Ad2-infected as compared to uninfected cells.

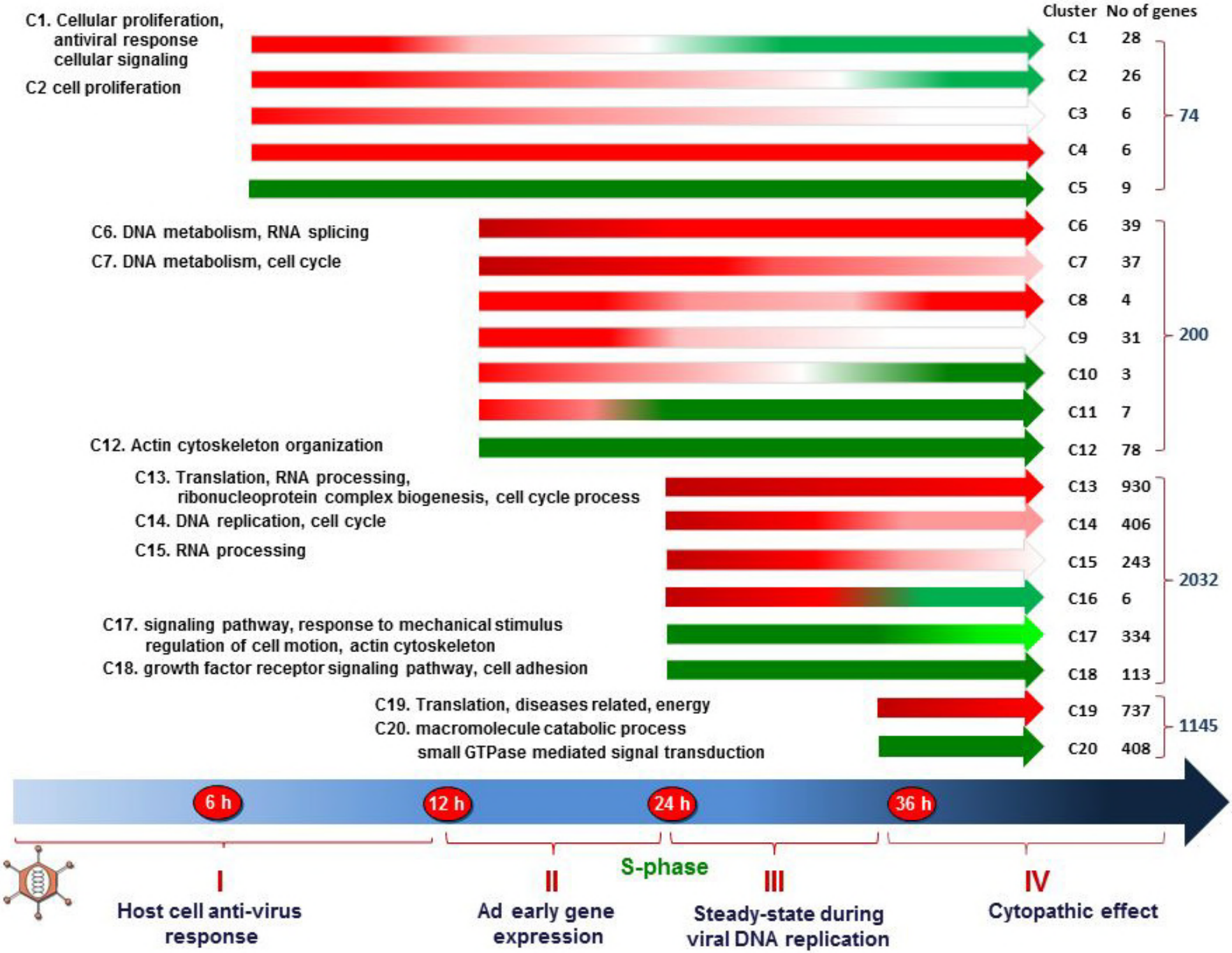
Cluster No of genes
C1. Cellular proliferation, antiviral response cellular signaling
C2 cell proliferation
C1 28
C2 26
C3 6
C4 6
C5 9
74
C6. DNA metabolism, RNA splicing
C7. DNA metabolism, cell cycle
C12. Actin cytoskeleton organization
C6 39
C7 37
C8 4
C9 31
C10 3
C11 7
C12 78
200
C13. Translation, RNA processing, ribonucleoprotein complex biogenesis, cell cycle process
C14. DNA replication, cell cycle
C15. RNA processing
C17. signaling pathway, response to mechanical stimulus regulation of cell motion, actin cytoskeleton
C18. growth factor receptor signaling pathway, cell adhesion
C13 930
C14 406
C15 243
C16 6
C17 334
C18 113
2032
C19. Translation, diseases related, energy
C20. macromolecule catabolic process small GTPase mediated signal transduction
C19 737
C20 408
1145
6 h
12 h
24 h
36 h
S-phase
I
Host cell anti-virus response
II
Ad early gene expression
III
Steady-state during viral DNA replication
IV
Cytopathic effect

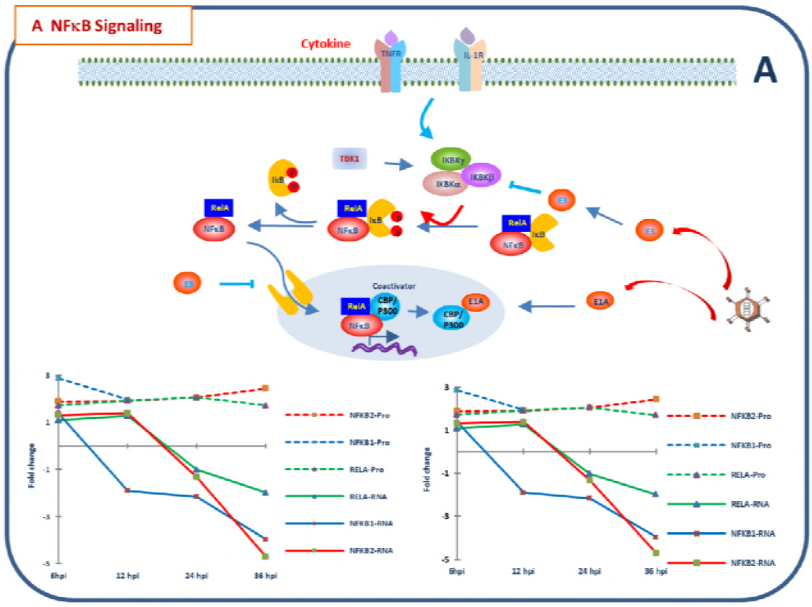
A NFκB Signaling
Cytokine
TNFR
IL 1R
A
TBK1
IKBKγ
IKBKα
IKBKβ
IκB
RelA
NFκB
E3
E1B
E1A
Coactivator
CBP/
P300
NFκB2-Pro
NFKB1-Pro
RELA-Pro
RELA-RNA
NFKB1-RNA
NFKB2-RNA
Fold change
6hpi
12 hpi
24 hpi
36 hpi

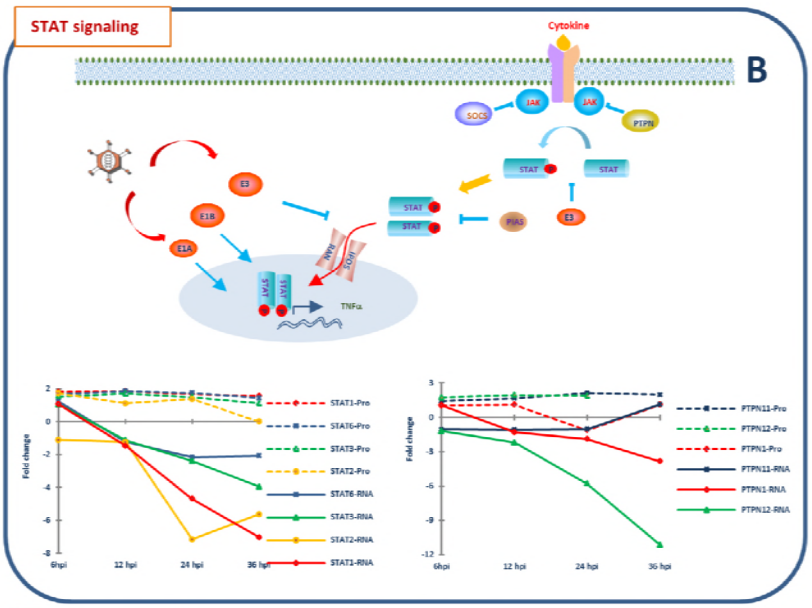
STAT signaling
Cytokine
B
JAK
SOCS
PTPN
STAT
PIAS
E3
E1B
E1A
NUC
TNFα
STAT1-Pro
STAT6-Pro
STAT3-Pro
STAT2-Pro
STAT6-RNA
STAT3-RNA
STAT2-RNA
STAT1-RNA
PTPN11-Pro
PTPN12-Pro
PTPN1-Pro
PTPN11-RNA
PTPN1-RNA
PTPN12-RNA
Fold change
6hpi
12 hpi
24 hpi
36 hpi

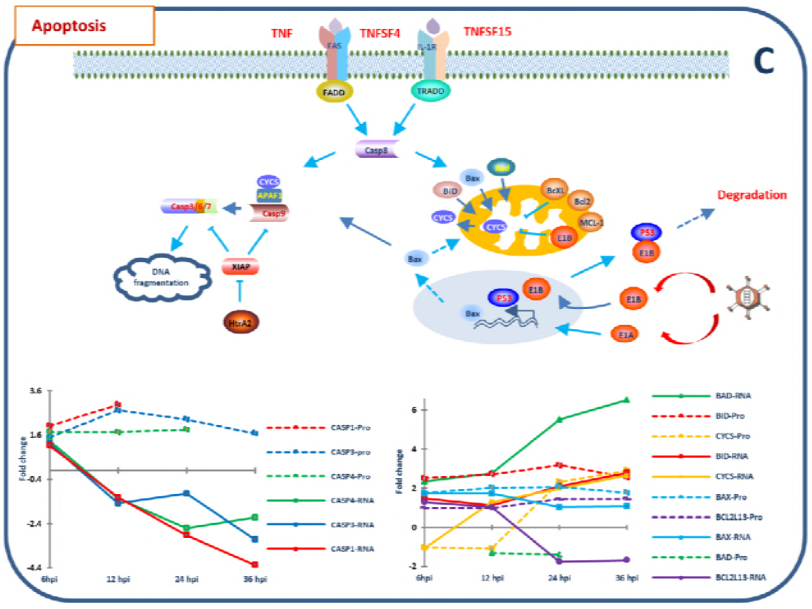
Apoptosis
TNF
TNFSF4
TNFSF15
C
FAS
IL-1R
FADD
TRADD
Casp8
Casp3/6/7
Casp9
CYCS
APAF1
DNA
fragmentation
XIAP
HtrA2
BID
Bax
Bcl2
BclXL
MCL1
CYCS
E1B
P53
Degradation
E1A
CASP1-Pro
CASP3-pro
CASP4-Pro
CASP4-RNA
CASP3-RNA
CASP1-RNA
BAD-RNA
BID-Pro
CYCS-Pro
BID-RNA
CYCS-RNA
BAX-Pro
BCL2L13-Pro
BAX-RNA
BAD-Pro
BCL2L13-RNA
Fold change
6hpi
12 hpi
24 hpi
36 hpi

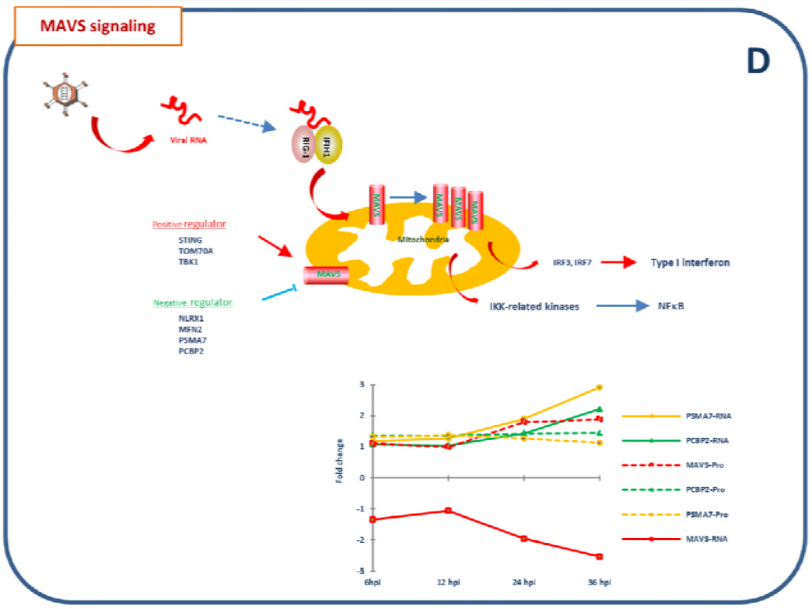
MAVS signaling
D
Viral RNA
RIG-I
IPS1
MAVS
Mitochondria
Positive regulator
STING
TOM70A
TBK1
Negative regulator
NLRX1
MFN2
PSMA7
PCBP2
IRF3, IRF7
Type I interferon
IKK-related kinases
NFκB
PSMA7-RNA
PCBP2-RNA
MAVS-Pro
PCBP2-Pro
PSMA7-Pro
MAVS-RNA
Fold change
6hpi
12 hpi
24 hpi
36 hpi

Table 2. Expressions of genes involved in cellular immune pathways at the RNA and protein levels (Up- and down-regulated RNAs or proteins were highlighted with red or green background).

Pathway	Entrez GeneID	Symbol	RNA expression									Protein expression							
			Seq Reads (RPKM)					Fold change				Fold change							
			Mock	Ad2-6h	Ad2-12h	Ad2-24h	Ad2-36h	Ad2-6h/M	Ad2-12h/M	Ad2-24h/M	Ad2-36h/M	Ad2-6h/M	Ad2-6h/M[a]	Ad2-12h/M	Ad2-12h/M	Ad2-24h/M	Ad2-24h/M	Ad2-36h/M	Ad2-36h/M
NFkB pathway	5966	REL	3,11	1,29	4,44	6,78	3,25	-2,41	1,43	2,18	1,04								
	5970	RELA	8,34	9,07	10,56	8,2	4,18	1,09	1,27	-1,02	-1,99	1,49	1,94	1,94	1,89	1,66	2,46	1,83	1,59
	5971	RELB	2,57	4,96	3,58	2,21	0,24	1,93	1,39	-1,17	-10,89								
	4790	NFKB1	23,98	32,77	12,61	11,09	6,03	1,37	-1,9	-2,16	-3,97		2,86	2,49	1,43				
	4791	NFKB2	7,76	10,13	10,81	5,85	1,65	1,31	1,39	-1,33	-4,71	1,88		1,96	1,85	2,13	1,97	2,44	
	4792	NFKBIA	27,49	50,03	39,55	10,73	2,58	1,82	1,44	-2,56	-10,66								
	4793	NFKBIB	2,96	3,5	5,4	23,03	50,04	1,18	1,83	7,79	16,93								
	4794	NFKBIE	3,02	2,43	1,7	0,48	0,42	-1,24	-1,77	-6,31	-7,19								
	64332	NFKBIZ	12,38	24,41	6,08	5,16	1,38	1,97	-2,04	-2,4	-8,97								
	3551	IKBKB	9,11	9,27	5,28	6,14	6,55	1,02	-1,73	-1,48	-1,39	1,71	1,68	1,75	1,6	1,37		1,72	1,41
	9641	IKBKE	3,86	4,55	2,2	0,21	0,16	1,18	-1,76	-18,14	-24,8								
	8517	IKBKG	8,83	8,22	7,72	3,31	2,86	-1,07	-1,14	-2,67	-3,09								
	29110	TBK1	15,46	15,62	14,59	18,34	3,68	1,01	-1,06	1,19	-4,2			1,37	-1,09	2,48	1,49	2,01	1,32
	121457	IKBIP	62,38	64,66	86,35	67,76	117,18	1,04	1,38	1,09	1,88	-1,1	-1,08	-1,16	-1,12	-1,12	-1,17	-1,31	
	8518	IKBKAP	17,63	12,99	24,1	28,2	24,4	-1,36	1,36	1,6	1,38	1,45			1,47	1,23	2,04	2,69	
STAT pathway	6772	STAT1	47,15	49,36	31,95	10,04	6,71	1,05	-1,48	-4,7	-7,02	1,56	2,03	1,8	1,89	1,64	1,66	1,79	1,32
	6773	STAT2	12,37	11,16	9,95	1,73	2,19	-1,11	-1,24	-7,15	-5,64	1,87	1,57	2,2			1,37		
	6774	STAT3	20,7	21,27	18,48	8,62	5,23	1,03	-1,12	-2,4	-3,95	1,54	1,49	1,79	1,62	1,34	1,64	1,2	-1,04
	6776	STAT5A	1,05	1,53	1,31	0,69	0,38	1,46	1,24	-1,53	-2,78								
	6777	STAT5B	8,18	6,84	6,43	3,92	2,94	-1,2	-1,27	-2,08	-2,78								
	6778	STAT6	15,13	18,39	12,39	6,96	7,24	1,22	-1,22	-2,17	-2,09	1,44	1,93	1,87	1,82	1,57	1,91	1,44	
	10379	IRF9	12,66	11,52	9,55	2,55	1,76	-1,1	-1,33	-4,97	-7,21								
	11099	JAK1	39,584	57,628	39	30,45	36,29	1,46	-1,02	-1,3	-1,09	-1,11	-1,09	-1,43	-1,24	1,65			
	3717	JAK2	12,928	9,601	20,03	2,39	2,67	-1,35	1,55	-5,42	-4,84								
	7297	TYK2	4,606	3,584	7,04	6,44	8,41	-1,29	1,53	1,4	1,83								
	10379	IRF9	12,66	11,52	9,55	2,55	1,76	-1,1	-1,33	-4,97	-7,21								
	79711	IPO4	8,37	11,34	14,38	18,45	27,93	1,35	1,72	2,2	3,33	1,3	1,94	1,83	1,91	2,21	2,71	3,11	2,61
	3843	IPO5	70,6	64,12	77,09	140,1	219,49	-1,1	1,09	1,98	3,11								
	10527	IPO7	81,4	76,2	68,65	88,61	56,74	-1,07	-1,19	1,09	-1,43	1,51	1,73	1,7	1,62	1,92	2,26	1,99	2,14
	10526	IPO8	11,77	8,17	11,68	6,02	2,99	-1,44	-1,01	-1,96	-3,94	1,39	1,38		1,28	1,35	1,51		1,01
	55705	IPO9	8,29	7,62	9,23	10,92	11,82	-1,09	1,11	1,32	1,43	1,81	2,11	2,14	1,92	1,62	2,09	1,77	1,44
	5901	RAN	218,35	243,71	271,63	610,2	752,62	1,12	1,24	2,79	3,45	1,56	1,86	2,13	1,88	2,12	2,09	2,03	1,84
	5770	PTPN1	29,58	31,19	23	15,66	7,69	1,05	-1,29	-1,89	-3,85	1,05	1,01	1,11	-1,08	-1,08	-1,2	1,06	-1,3
	5771	PTPN2	11,56	14,23	14,25	8,87	5,48	1,23	1,23	-1,3	-2,11								
	5780	PTPN9	16,03	15,26	15,05	12,07	5,35	-1,05	-1,07	-1,33	-3								
	5781	PTPN11	107,55	101,5	98,71	103,4	121,24	-1,06	-1,09	-1,04	1,13	-1,04	1,82	1,66	1,68	1,91	2,32	2,27	1,68
	5782	PTPN12	28,93	24,12	13,15	5	2,6	-1,2	-2,2	-5,79	-11,14	1,74		1,71	2,18	1,54	2,24		
	5783	PTPN13	9,93	8,53	12,35	5,85	4,33	-1,16	1,24	-1,7	-2,29								
	5784	PTPN14	28,65	20,22	11,72	3,63	2,14	-1,42	-2,45	-7,88	-13,39								
	26469	PTPN21	12,43	11,43	5,8	1,73	0,96	-1,09	-2,14	-7,18	-12,94								
	6714	SRC	1,64	1,82	1,77	3,04	0,72	1,11	1,08	1,85	-2,78					-1,14	1,11	1,10	-1,22
Apoptosis	9966	TNFSF15	3,25	22,25	1,23	0,13	0,36	6,85	-2,65	-25,14	-8,91								
	7292	TNFSF4	13,65	11,23	2,78	0,71	-	-1,22	-4,92	-19,28	-13,65	-1,12	-1,18						
	4982	TNFRSF11B	264,00	338,58	100,00	10,67	10,15	1,28	-2,64	-24,75	-26,02								
	51330	TNFRSF12A	154,04	189,38	108,11	23,96	25,90	1,23	-1,42	-6,43	-5,95								
	8793	TNFRSF10D	63,81	81,21	100,23	109,03	167,85	1,27	1,57	1,71	2,63								
	8795	TNFRSF10B	36,50	58,73	54,58	45,47	44,50	1,61	1,50	1,25	1,22								
	55504	TNFRSF19	15,97	12,01	15,13	6,37	6,00	-1,33	-1,06	-2,51	-2,66								
	7132	TNFRSF1A	15,99	23,77	18,27	5,92	1,80	1,49	1,14	-2,70	-8,87								
	7133	TNFRSF1B	2,53	2,93	1,90	4,13	5,01	1,16	-1,33	1,63	1,98								
	27242	TNFRSF21	7,01	6,49	6,71	2,50	2,30	-1,08	-1,04	-2,80	-3,05								
	355	FAS	29,00	32,62	29,42	23,35	27,09	1,12	1,01	-1,24	-1,07								
	8797	TNFRSF10A	0,64	1,78	2,56	6,94	8,00	2,77	3,98	10,81	12,46								
	7186	TRAF2	2,45	1,66	2,63	2,7	2,58	-1,48	1,07	1,1	1,05								2,41
	10131	TRAP1	14,67	14,53	26,94	57,12	83,3	-1,01	1,84	3,89	5,68	-1,05	-1,1	-1,13	-1,1	1,13	1,17	1,35	1,33
	598	BCL2L1	14,76	15,24	8,1	3,22	1,48	1,03	-1,82	-4,59	-10								
	23786	BCL2L13	19,51	25,36	20,22	11,06	11,61	1,3	1,04	-1,76	-1,68	1,24	-1,14	-1,36	-1,02		1,45	1,47	
	599	BCL2L2	11,5	12,4	11,11	15,34	15,44	1,08	-1,03	1,33	1,34								
	4170	MCL1	96,6	144,5	87,54	60,8	35,69	1,5	-1,1	-1,59	-2,71								
	581	BAX	7,43	12,83	12,83	7,69	8	1,73	1,73	1,04	1,08	1,64	1,89	2,27	1,79	2,17	2	2,18	1,36
	637	BID	15,54	22,96	17,53	32,71	43,46	1,48	1,13	2,1	2,8	1,88	3,13	2,64	2,8	2,91	3,44	2,79	2,35
	572	BAD	1,5	3,53	4,16	8,28	9,81	2,34	2,77	5,51	6,52			-1,35	-1,31	-1,31	-1,45		
	573	BAG1	5,64	6,36	9,26	13,21	19,28	1,13	1,64	2,34	3,42								
	9532	BAG2	10,35	9,8	8,06	7,47	5,18	-1,06	-1,28	-1,39	-2	-1,09	1,02	-1,11	1,04	1,04	-1,01	1,12	-1,11
	9531	BAG3	8,16	9,16	7,75	8,44	4,57	1,12	-1,05	1,03	-1,78		1,63	1,77	1,61	3,13	3,03	3,6	
	9530	BAG4	16,92	14,3	17,17	12,1	10,24	-1,18	1,02	-1,4	-1,65								
	9529	BAG5	16,42	15,16	15,56	22,07	8,35	-1,08	-1,06	1,34	-1,97								
	7917	BAG6	10,57	10,4	11,5	7,75	13,6	-1,02	1,09	-1,36	1,29								
	54205	CYCS	69,59	65,88	90,45	139,01	184,24	-1,06	1,30	2,00	2,65	-1,01	-1,03	-1,13	-1,03	3,05	1,61	3,87	1,95
	834	CASP1	19,65	22,47	16,12	6,71	4,58	1,14	-1,22	-2,93	-4,29	2,02		2,99		2,93	3,14		
	835	CASP2	3,5	1,48	4,7	6,01	1,79	-2,37	1,34	1,72	-1,95								
	836	CASP3	50,96	62,1	34,29	48,89	16,35	1,22	-1,49	-1,04	-3,12	1,49		2,92	2,54	1,95	2,69	1,72	1,63
	837	CASP4	80,5	108,96	64,46	30,83	37,74	1,35	-1,25	-2,61	-2,13	1,27	2,23	1,53	1,95	2	1,71		
	839	CASP6	5,45	4,79	8,89	9,08	7,84	-1,14	1,63	1,67	1,44								
	840	CASP7	9,37	12,92	12,6	19,61	9,81	1,38	1,34	2,09	1,05								
	841	CASP8	6,68	5,52	4,3	4,34	3,6	-1,21	-1,55	-1,54	-1,85								
	9994	CASP8AP2	11,31	7,88	16,64	15,96	4,38	-1,43	1,47	1,41	-2,58								
	790	CAD	3,29	3,799	6,14	6,08	4,23	1,15	1,86	1,85	1,28	1,2	1,2	1,51	1,62	1,33	2,21	1,59	2,2
	7157	TP53	8,19	7,39	5,89	9,1	15,47	-1,11	-1,39	1,11	1,89								
	7158	TP53BP1	18,87	15,85	23,88	6,55	2,26	-1,19	1,27	-2,88	-8,33	1,16	1,16	1,12	1	1,08	1,11	1,03	-1,02
	7159	TP53BP2	15,22	16,12	16,79	9,5	6,16	1,06	1,1	-1,6	-2,47								
	112858	TP53RK	12,49	12,92	14,16	4,2	2,89	1,03	1,13	-2,97	-4,33			1,32	1,07	1,5		1,33	
	329	BIRC2	59,44	75,94	39,41	13,31	15,26	1,28	-1,51	-4,46	-3,9								
	330	BIRC3	5,02	13,05	2,88	1,37	0,72	2,6	-1,74	-3,67	-6,92								
	332	BIRC5	1,39	1,92	1,61	17,94	33,88	1,39	1,16	12,94	24,45								
	57448	BIRC6	41,06	32,36	37,58	15,78	11,23	-1,27	-1,09	-2,6	-3,66								
	331	XIAP	16,57	15,62	13,33	6,27	6,03	-1,06	-1,24	-2,64	-2,75								
MAVS	5688	PSMA7	93,32	110,46	118,29	176,88	272,83	1,18	1,27	1,9	2,92	1,33	1,33	1,36	1,39	1,36	1,19	1,21	1,05
	5094	PCBP2	28,42	30,77	27,23	40,7	63,18	1,08	-1,04	1,43	2,22	1,37	1,37	1,47	1,26	1,34	1,54	1,97	-1,02
	57506	MAVS	4,35	3,25	4,1	2,22	1,72	-1,34	-1,06	-1,95	-2,53	1,11	1,11	1,24	-1,24	1,76	1,86	2,63	1,15

[a]Biological replicates